Cancer Letters 467 (2019) 72–84

Contents lists available at ScienceDirect

Cancer Letters

journal homepage: www.elsevier.com/locate/canlet

Original Articles

Aromatase-induced endogenous estrogen promotes tumour metastasis through estrogen receptor-α/matrix metalloproteinase 12 axis activation in castration-resistant prostate cancer

Zhixian Liang[a,1], Jiasong Cao[a,1], Lei Tian[a], Yongmei Shen[a], Xu Yang[a], Qimei Lin[a], Ran Zhang[a], Haitao Liu[b], Xiaoling Du[a], Jiandang Shi[a,*], Ju Zhang[a,**]

[a] Department of Biochemistry and Molecular Biology, College of Life Sciences, Bioactive Materials Key Lab of the Ministry of Education, Nankai University, Tianjin, 300071, China

[b] Shanghai First People's Hospital Shanghai Jiaotong University, Shanghai, 200080, China

ARTICLE INFO

Keywords:
CYP19A1
Endogenous estrogenic effects
CD44
MMP12
Androgen independence prostate cancer

ABSTRACT

Castration-resistant prostate cancer (CRPC) following androgen deprivation therapy remains a major obstacle advanced prostate cancer management. Aromatase catalyzes estrogen from androgens, yet the role of aromatase-generated endogenous estrogen in CRPC is poorly understood. In this study, we assessed the expression and function of aromatase in CRPC. We found that aromatase expression was significantly increased in CRPC tissues and cell lines. In some prostate cancer cell lines, aromatase was predominantly expressed in $CD44^+$ subsets. Bicalutamide treatment significantly increased aromatase expression, and *CYP19A1* expression positively correlated with estrogen responses and epithelial-mesenchymal transition. Aromatase knockdown in PC3 cells reduced invasiveness and decreased metastasis-related gene expression. The aromatase inhibitor, letrozole, attenuated tumour metastasis in castrated PC3-xenograft mice. Mechanistically, aromatase-induced endogenous estrogen promoted estrogen receptor-α (ERα) binding to matrix metalloproteinase 12 (MMP12) promoter estrogen response element (ERE). MMP12 co-localized with CD44 on the cell membrane and MMP12 knockdown significantly reduced estradiol-induced PC3 invasion. Taken together, our findings indicated that increased endogenous estrogen, catalysed by elevated aromatase levels, enhanced MMP12 expression via ERα, participated in CRPC progression and promoted tumour metastasis. Thus, aromatase represents a potential novel therapeutic target for CRPC.

1. Introduction

Prostate cancer (PCa) is the most common cancer and the second leading cause of cancer death in men in the United States [1]. The standard therapy for locally advanced or metastatic PCa is androgen deprivation therapy (ADT) [2], which inhibits androgen synthesis or impedes androgen receptor (AR) signalling through surgical or chemical castration using gonadotropin-releasing hormone agonists or antagonists and AR antagonists (such as flutamide, bicalutamide and MDV3100) [3,4]. Although initially effective at blocking tumour growth, this approach frequently fails, and the disease progresses to castrate-resistant prostate cancer (CRPC), which continues to be a major clinical challenge [5,6].

Previous studies identified several mechanisms that induce CRPC, including AR signalling restoration, AR bypass signalling, and complete AR independence [7–9]. In addition, cumulative evidence supports the important role of prostate cancer stem-like cells (PCSLCs) during CRPC development [10–12]. In fact, these cells are much more resistant to androgen deprivation than non-PCSLCs because they are considered insensitive to androgen [13]. In particular, PCSLCs are reportedly equipped with classical (α and β) and novel (GPR30) estradiol receptors (ERs), which play an important role in cancer proliferation, migration and prostaspheres [14].

Increasing evidence suggests that estrogens are associated with the progression of PCa [15–17]. The concentration of 17β-estradiol in prostatic fluids appears to be significantly higher in PCa patients than in

* Corresponding author.
** Corresponding author.
E-mail addresses: shijd@nankai.edu.cn (J. Shi), zhangju@nankai.edu.cn (J. Zhang).
[1] These authors contributed equally to this work.

https://doi.org/10.1016/j.canlet.2019.09.001
Received 30 June 2019; Received in revised form 17 August 2019; Accepted 4 September 2019

healthy volunteers of a similar age [18]. Estrogen receptor alpha (ERα) is reportedly involved in PCa progression by regulating nuclear-enriched abundant transcript 1 and TMPRSS2-ERG fusion [19,20]. Aromatase (CYP19A1) is the key enzyme in the metabolism of testosterone and androstenedione to estrone and estradiol, and it directly regulates the local balance of androgen conversion to estrogens [15]. Aromatase is also a crucial therapeutic target in the clinical treatment of breast cancer [21]. In the prostate, aromatase is more effective in PCa than in benign prostatic hyperplasia [22]. Chronically increased estrogen and aromatase levels have been linked to an increased risk of PCa [23]. It has been reported that aromatase promotes the metastatic homing and growth of PCSLC in the bone marrow [24]. However, the mechanisms of aromatase and estrogen signalling involved in the progression of PCa, especially CRPC, remain largely unknown.

CD44 is a hyaluronan-binding cell surface glycoprotein that is often used to purify cancer stem cells from breast, head and neck, ovarian, liver and PCa tumours [25,26]. CD44(+) PCa cells from xenograft prostate human tumours are more proliferative, clonogenic, tumourigenic, and metastatic than isogenic CD44(−) PCa cells, and they possess certain stemness properties [27]. Additionally, CD44 has been shown to be a key driver in prostate cancer stem cells associated with chemoresistance [28].

Metastasis is frequently the cause of cancer-related death in PCa [29]. Matrix metalloproteinase (MMP) family members are involved in the metastasis of various cancers [30]. MMP12, also known as macrophage metalloelastase, is believed to promote cancer invasion in glioma and nasopharyngeal adenocarcinoma [31,32]. In the prostate, MMP12 was shown to be involved in the interactions between PCa cells and bone marrow stromal cells during bone metastasis [33].

In this study, we investigate the role of aromatase in CRPC. We report that aromatase overexpression in CRPC is associated with an increased number of $CD44^+$ PCa cells and promotes tumour metastasis by upregulating MMP12.

2. Materials and methods

2.1. Bioinformatics analysis

Ross-Adams (GSE70770) [34], Tomlins (GSE6099) [35], and Yu (GSE6919) [36] datasets from the National Center for Biotechnology Information (NCBI) Gene Expression Omnibus (GEO) database (http://www.ncbi.nlm.nih.gov/geo/) and the Grasso dataset [37] from Oncomine (Life Technologies, http://www.oncomine.org/) were used in our study. The Cancer Genome Atlas Prostate Adenocarcinoma (TCGA-PRAD) cohort datasets, including 498 prostate tumour tissues and 52 adjacent normal tissues, were obtained from the Genomic Data Commons Data Portal (https://portal.gdc.cancer.gov/). The normalization procedure was performed according to the log2(1 + x) and Z-score methods, and a differential expression analysis with the highest versus lowest CYP19A1 expression values (top and bottom 10% from the TCGA dataset) [38] was then performed using edgeR [39]. Heatmaps and hierarchical clustering were generated using Morpheus (https://software.broadinstitute.org/morpheus). gene set enrichment analysis (GSEA) analyses were performed using the GSEA software package (GSEA-3.0.jar) and molecular signatures available from the Broad Institute [40]. Clinical outcome analyses, including Kaplan-Meier analyses, were performed using GraphPad Prism (v8) software.

2.2. Immunohistochemistry (IHC) and immunofluorescence (IF) analyses

Benign prostate tissue from patients undergoing radical cystectomy (age 53–67, $n = 21$) was obtained from the Department of Urology, Shanghai First People's Hospital, Shanghai, China. Primary PCa tissue from patients undergoing radical prostatectomy (age 63–78, $n = 34$) and CRPC tissue from patients undergoing channel transurethral resection of the prostate (age 63–78, $n = 28$) were obtained from the Department of Urology, Third Central Hospital, Tianjin, China. All samples were obtained with the informed consent of the patients, and approval of the study was obtained from the Ethics Committee of Nankai University.

IHC and IF were performed on prostate tissues as previously described [41]. For IF analysis of prostate cancer cells, LNCaP cells with or without bicalutamide treatment and PC3 cells were seeded on coverslips in 24-well culture plates for 48 h. Then, the cells were fixed with 4% paraformaldehyde and analysed as described previously [42]. IHC images were taken using an Olympus microscope BX43 (Olympus, Tokyo, Japan) at 100 × and 400 × magnification; IF images were taken using a Zeiss LSM710 confocal microscope (Germany) at 200 ×, 400 × and 630 × magnification. The staining intensity of the IHC images was determined as the average optical density using Image-Pro Plus 6.0 software (Media Cybernetics, Bethesda, MD, USA) as described previously [43].

2.3. Cell culture and bicalutamide treatment

The prostate cancer cell lines LNCaP and LNCaP abl were a kind gift from Helmut Klocker (Department of Urology of Medical University of Innsbruck, Austria), and the prostate cancer cell line PC3 was a kind gift from Doris Mayer (German Cancer Research Center, DKFZ, Germany). LNCaP and PC3 cells were cultured in RPMI 1640 medium (Gibco, Grand Island, NY, USA) supplemented with 1% penicillin/streptomycin (P/S, HyClone, Logan, UT, USA) and 10% foetal bovine serum (FBS; Gibco). LNCaP abl cells were cultured in RPMI 1640 medium supplemented with 1% P/S and 10% charcoal-stripped FBS (CS-FBS, Omega, Tarzana, CA). LNCaP, LNCaP abl and PC3 cells were treated with 20 μM bicalutamide (Selleck Chemicals, Houston, Texas, USA) for 7 days. LNCaP abl cells were treated with testosterone (Sigma-Aldrich, Saint Louis, MI, USA) or 17β-estradiol (Sigma-Aldrich) at a concentration of 10 nM. Bicalutamide, testosterone and 17β-estradiol were dissolved in DMSO.

2.4. Western blotting and quantitative RT-PCR

After receiving the indicated treatments, cells were collected and lysed for protein isolation and RNA extraction as described previously [44,45]. Antibodies against aromatase (HPA051194; Sigma-Aldrich), CD44 (ab6124, Abcam, Cambridge, MA, USA), MMP12 (ab52897, Abcam), ERα (ab32063, Abcam), AR (M3562, Dako, California, USA) and GAPDH (KC-5G4, KANGCHEN, China) were used. Specific primer pairs for *CYP19A1*, *CD44*, *MMP12*, *ERα*, *AR*, *HPRT* and metastasis-related genes are listed in Table S1.

2.5. Analysis and collection of $CD44^+$ and $CD44^-$ subsets of prostate cancer cell lines by fluorescence-activated cell sorting (FACS)

LNCaP and LNCaP abl cells were resuspended in 0.1% BSA-Hank's balanced salt solution and labelled with CD44-APC (4312475, Affymetrix eBioscience, San Diego, CA, USA). A small fraction without antibody was used to delineate the unstained and autofluorescent populations. The fluorescence intensity of the cells was quantified, and $CD44^+$ and $CD44^-$ subsets were sorted by a flow cytometer (BD FACSAria III, USA).

2.6. Plasmid, siRNA and lentiviral transfection

The CYP19A1-pENTER plasmid was purchased from ViGene Biosciences Inc. (MD, USA), and siRNAs targeting CYP19A1 or MMP12 and a negative control siRNA that did not match any known human cDNA were purchased from GenePharma (Shanghai, China). The siRNA sequences used are listed in Table S2. The plasmid and siRNA transfection procedures have been described previously [41]. PC3-ZsGreen cells were obtained by lentiviral transfection. The pLVX-ZsGreen-Puro

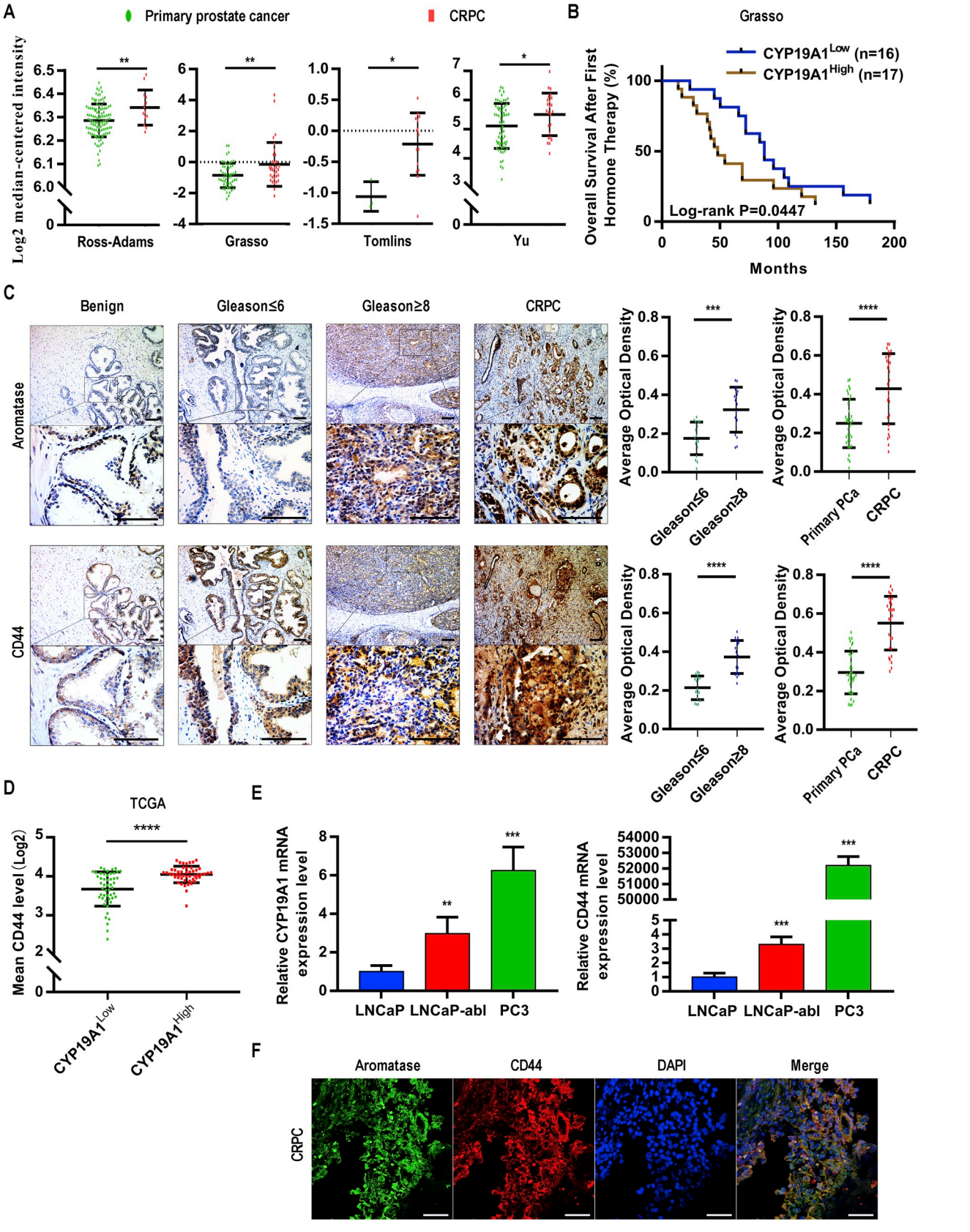

(caption on next page)

Fig. 1. Expression of aromatase and CD44 in PCa. (A) Scatter dot plots present aromatase mRNA expression in primary tumour and CRPC tissues from 4 publicly available datasets (*t*-test). (B) Kaplan-Meier analysis shows the overall survival of CYP19A1^{High} samples vs. CYP19A1^{Low} samples in the Grasso dataset after initial hormone therapy. (C) Immunohistochemical analysis of aromatase and CD44 in benign prostate (n = 21), low Gleason score (Gleason score ≤ 6) PCa tumour (n = 17), high Gleason score (Gleason score ≥ 8) PCa tumour (n = 17) and CRPC tissues (n = 28); representative microphotographs are shown; scale bar: 100 μm. The right panel shows the average optical density of aromatase and CD44 for low Gleason score vs. high Gleason score tissues and primary tumour vs. CRPC tissues (*t*-test). (D) Mean mRNA analysis of *CD44* for CYP19A1^{High} samples vs. CYP19A1^{Low} samples in prostate adenocarcinoma (PRAD) from the cancer genome atlas (TCGA). (E) The mRNA levels of *CYP19A1* (left panel) and *CD44* (right panel) in LNCaP, LNCaP abl and PC3 cells are shown (one-way ANOVA). (F) Representative immunofluorescence graphs of aromatase and CD44 in CRPC tissues, scale bar: 50 μm. The average optical density was measured by Image-Pro Plus 6.0 software; the values are the means ± SE; $^{*}P < 0.05$, $^{**}P < 0.01$, $^{***}P < 0.001$, $^{****}P < 0.0001$.

plasmid was transfected into 293T packaging cells with Optimized Packaging Mix. Then, pseudotyped lentiviral particles were used to infect PC3 cells. After selection with puromycin, PC3-ZsGreen cells were used for the *in vivo* studies.

2.7. Luciferase assay and high-performance liquid chromatography-mass spectrometry (HPLC-MS) for evaluating the estrogenic effects in prostate cancer cells

PGL3-$(ERE)_6$-luciferase reporter (ERE-luc) and PGL3-AROM-promoter-luciferase reporter (AROM-pro-luc) plasmids were transfected into prostate cancer cells after the indicated treatment for 24 h. Then, the luciferase activity was detected using a Dual-Glo luciferase assay kit (Promega, Madison, WI, USA) as described previously [46]. 17β-estradiol levels in LNCaP, LNCaP abl and PC3 cells were determined by HPLC-MS. We counted the number of cells, and 10^6 cells were resuspended in 1 mL of PBS. Then, the samples were prepared as described [47]. Liquid chromatography-tandem mass spectrometry (LCMS-2020, SHIMADZU, Japan) was used to evaluate the level of 17β-estradiol in the samples. The monitored ion of 17β-estradiol on the mass spectra was at 506 *m/z*, and the retention time was 5.7 min (Fig. S1). The limit of detection (LOD) was 0.045 ng/mL, and the limit of quantification (LOQ) was 0.149 ng/mL.

2.8. Chromatin immunoprecipitation (ChIP) and co-immunoprecipitation (Co-IP) assays

PC3 cells were seeded in 100-mm dishes and treated with DMSO or 10 nM 17β-estradiol for 1 h before harvest. ChIP assays were performed as described previously [48]. The primers used in the ChIP assays are shown in Table S1, and an ERα antibody (ab32063, Abcam) was used. For Co-IP assays, whole cell lysates were prepared by lysing cells in NP-40 cell lysis buffer with 1 mM PMSF (Solarbio, Beijing, China). The cell lysates were pre-incubated with a CD44 antibody (ab6124, Abcam) or IgG (bs-0296P, Bioss, China) as a negative control for 30 min. Then, the samples were incubated with Dynabeads™ magnetic beads (10004D, Invitrogen, Carlsbad, CA, USA) on a rotator at 4 °C for 2 h. Finally, the samples were washed 5 times with wash buffer and resuspended for western analysis.

2.9. Matrigel invasion assay

Transwell assays were used to evaluate the invasive capability of PC3 cells. Briefly, 80 μL of RPMI 1640 medium with 20 μL of Matrigel (Corning, Bedford, MA USA) was added to transwell migration chambers (Transparent PET Membrane 24-well, 8.0-μm pore size, Corning, NY, USA), and 500 μL of RPMI 1640 medium supplemented with 10% FBS was added to the lower wells. Then, PC3 cells were seeded in the upper chambers at 50 000 cells per well in RPMI 1640 serum-free medium. After an overnight incubation, the cells that had migrated through the filter to the lower surface were fixed with 4% paraformaldehyde and stained with a 0.5% crystal violet solution (BBI, Shanghai, China). Finally, the cells from five randomly selected fields per chamber were counted.

2.10. Xenograft mouse model

A total of 45 BALB/c athymic SCID nude male mice aged 8–12 weeks (18–20 g body weight, obtained from Weitong-Lihua Experimental Animal, Beijing, China) were kept in an animal facility under standard laboratory conditions. Animal care and experiments were conducted in accordance with the guidelines of the Chinese Council on Animal Care and approved by the Nankai University Animal Care and Use Committee.

The mice were castrated, and PC3-ZsGreen cell suspensions (10^6 PC3-ZsGreen cells suspended in 100 μL of RPMI 1640 serum-free medium mixed with 100 μL of Matrigel) were inoculated subcutaneously into the primary prostate of the mice. After 1 week, the mice were randomized into 5 groups and treated according to different protocols: 1) castration only (Ctrl), 2) castration plus testosterone (T), 3) castration plus 17β-estradiol (E2), 4) castration plus the aromatase inhibitor letrozole (LE), 5) castration plus testosterone plus letrozole (LE + T). For administration, testosterone and 17β-estradiol were dissolved in 0.1 mL of corn oil tightly packed into silicone tubes as previously described [49,50]. Letrozole (MCE, USA) was administered by intraperitoneal injection at 10 μg/day for 30 days. Then, the mice were weighed, euthanized and dissected to harvest the primary tumours and metastases. An *in vivo* imaging device, the IVIS imaging system (IVIS Lumina II, Xenogen, USA), was used for analyses.

2.11. Statistical analysis

SPSS 22.0 and GraphPad Prism (v8) were used for statistical analyses. Student's *t*-test was used for analysing differences between two groups, and more than two groups were compared with one-way ANOVA. $P < 0.05$ was considered significant.

3. Results

3.1. CYP19A1 expression is increased and co-expressed with CD44 in CRPC tissue

We examined the expression of *CYP19A1* in primary PCa and CRPC tissues from 4 publicly available datasets (Ross-Adams, 112 primary PCa and 13 CRPC samples; Grasso, 52 primary PCa and 33 CRPC samples; Tomlins, 3 primary PCa and 15 CRPC samples; Yu, 64 primary PCa and 24 CRPC samples). *CYP19A1* expression was significantly higher in CRPC than in primary PCa (Fig. 1A). In addition, a subset of patients with higher *CYP19A1* expression suffered poorer overall survival after first hormone therapy compared with those with lower *CYP19A1* expression (Fig. 1B). Next, immunohistochemical analysis was performed to evaluate the protein expression of aromatase and CD44 in benign prostate (n = 21), primary PCa (n = 34) and CRPC (n = 28) samples. In the benign prostate samples, aromatase and CD44 immunoreactivity was detected in some basal epithelial cells. In the primary PCa samples, we detected that high Gleason score (Gleason score ≥ 8) tumours had stronger aromatase and CD44 staining than low Gleason score (Gleason score ≤ 6) tumours (Fig. 1C). The CRPC samples displayed higher aromatase and CD44 expression than the primary PCa samples. (Fig. 1C). Then, we selected the top 10% of CYP19A1^{High} and CYP19A1^{Low} prostate adenocarcinoma samples individually from

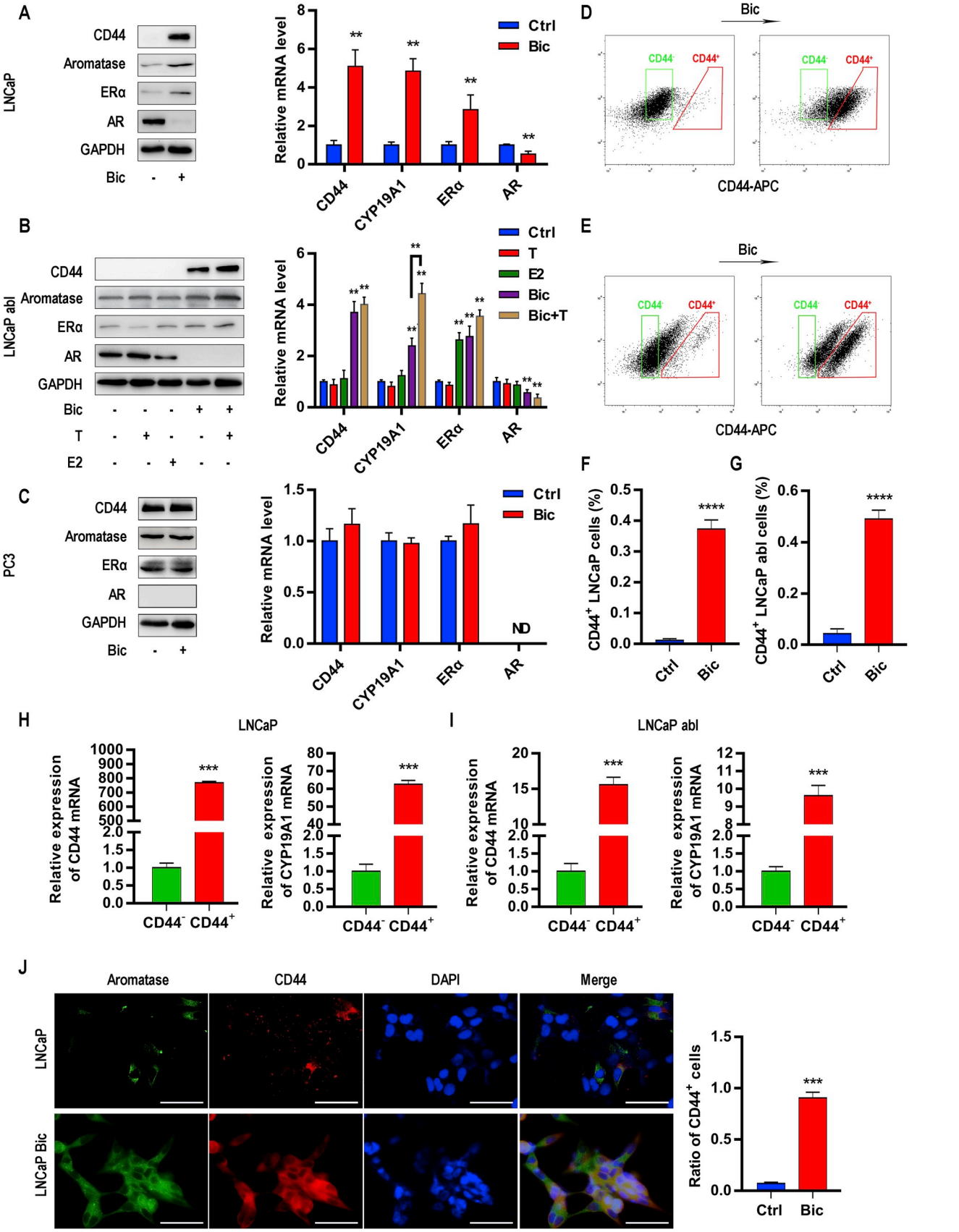

(caption on next page)

Fig. 2. Effect of bicalutamide treatment on LNCaP, LNCaP abl and PC3 cells. LNCaP, LNCaP abl and PC3 cells were treated with 20 μM bicalutamide (Bic) for 7 days, and LNCaP abl cells were exposed to 10 nM testosterone (T) or 17β-estradiol (E2). (A–C) The protein (left panel) and mRNA (right panel) levels of aromatase, CD44, ERα and AR (LNCaP cells, A, *t*-test; LNCaP abl cells, B, one-way ANOVA; PC3 cells, C, *t*-test) were analysed. (D and E) Representative FACS plots of $CD44^+$ vs. $CD44^-$ cells before and after bicalutamide treatment in LNCaP (D) and LNCaP abl (E) cells are shown. (F and G) The percentage of $CD44^+$ cells before and after bicalutamide treatment in LNCaP (F) and LNCaP abl (G) cells are shown (*t*-test). (H and I) *CD44* and *CYP19A1* expression in $CD44^+$ vs. $CD44^-$ subsets of LNCaP (H) and LNCaP abl (I) cells according to RT-PCR (*t*-test). (J) Representative immunofluorescence graphs of aromatase and CD44 in LNCaP cells before and after bicalutamide treatment; scale bar: 50 μm; the right panel shows the ratio of $CD44^+$ cells. All studies were repeated at least three times; the values are the means ± SE; $^{**}P < 0.01$, $^{***}P < 0.001$, $^{****}P < 0.0001$, ND, not detected.

TCGA, and the mean expression of the CD44 gene was significantly higher in $CYP19A1^{High}$ prostate adenocarcinoma samples than in $CYP19A1^{Low}$ prostate adenocarcinoma samples (Fig. 1D). In addition, androgen-independent PCa cell lines (LNCaP abl and PC3) showed significantly higher mRNA levels of *CYP19A1* and *CD44* expression than androgen-dependent PCa cell line (LNCaP, Fig. 1E). Moreover, CD44 and aromatase showed good co-expression in CRPC tissue according to confocal microscopy (Fig. 1F).

3.2. *CYP19A1* expression was increased and associated with an increased proportion of $CD44^+$ stem-like cells after bicalutamide treatment

To identify aberrant aromatase expression during CRPC development, we cultured LNCaP, LNCaP abl and PC3 cell lines and treated them with an AR blocker, bicalutamide, which is frequently used for ADT. After 7 days of exposure to 20 μM bicalutamide, we detected a significant increase in aromatase and CD44, along with higher ERα and lower AR in LNCaP cells at the mRNA and protein levels (Fig. 2A). Because LNCaP abl cells are already adapted to grow in steroid-ablated conditions, we also treated these cells with 10 nM exogenous testosterone or 17β-estradiol to investigate the expression of aromatase after bicalutamide treatment. Similarly, aromatase, CD44 and ERα expression levels were significantly increased, and AR expression was significantly decreased after short-term bicalutamide treatment in the LNCaP abl cell line (Fig. 2B), which is sensitive to bicalutamide although it is an androgen-insensitive PCa cell line [51]. In addition, we detected a significant increase in aromatase expression following treatment with testosterone in AR-blocking conditions (Fig. 2B). However, PC3 cells lacking AR showed no significant changes upon bicalutamide treatment, but they expressed high levels of aromatase, CD44 and ERα (Fig. 2C).

We next sorted $CD44^+$ and $CD44^-$ subsets of LNCaP and LNCaP abl cells by FACS (Fig. 2D–E). We observed significantly higher expression of prostate cancer stem-like markers and metastasis-related genes in $CD44^+$ cells than in $CD44^-$ cells (Fig. S2). *CYP19A1* expression was significantly higher in $CD44^+$ cells than in $CD44^-$ cells in both LNCaP and LNCaP abl cell lines (Fig. 2H–I). In addition, the ratio of $CD44^+$ subsets was significantly higher in the LNCaP and LNCaP abl cell lines after bicalutamide treatment (LNCaP 37.3% ± L.96%; LNCaP abl 49.0% ± 9.51%) than in the control cells (LNCaP 1.15% ± (0.52%, Fig. 2D–F; LNCaP abl 4.34% ± 0.83%, Fig. 2E–G). Using an IF assay, we further investigated the relationship between CD44 and aromatase expression in LNCaP cells. Good co-expression of aromatase and CD44 was observed in LNCaP cells, similar to the finding in CRPC tissue. In addition, the frequency of $CD44^+$ LNCaP cells with a high level of aromatase was increased after bicalutamide treatment (Fig. 2J). Together, these data suggest that $CD44^+$ stem-like cells with high aromatase expression were increased after AR blockade.

3.3. ER transcriptional activity was enhanced in association with aromatase upregulation upon bicalutamide treatment

Since aromatase is increased dramatically during bicalutamide treatment, we next investigated the activity of estrogen under androgen depletion conditions. The Dual-Luciferase® Reporter (DLR™) Assay System was used to evaluate the relative activity of the *CYP19A1* promoter (AROM-pro-luc) and estrogen response element (ERE-luc) in LNCaP and LNCaP abl cells upon bicalutamide treatment. In LNCaP cells, the *CYP19A1* promoter and ER transcriptional activity were significantly increased (Fig. 3A–C). In LNCaP abl cells, bicalutamide significantly increased the activity of the *CYP19A1* promoter (Fig. 3B); on the other hand, ER transcriptional activity was enhanced significantly upon bicalutamide treatment in the presence of testosterone, as well as upon 17β-estradiol treatment (Fig. 3D).

To verify the relationship between aromatase expression and the estrogenic effect, we conducted GSEA between $CYP19A1^{High}$ and $CYP19A1^{Low}$ prostate adenocarcinoma samples from the TCGA dataset. These results revealed that *CYP19A1* expression was positively correlated with signatures representative of the early estrogen response (Fig. 3E). In addition, the mean expression of estradiol receptors (estradiol receptors α and β and GPR30) was significantly higher in $CYP19A1^{High}$ prostate adenocarcinoma samples than in $CYP19A1^{Low}$ prostate adenocarcinoma samples (Fig. 3F). Then, we cultured PC3 cells under hormone-free conditions (CS-FBS), treated them with testosterone and evaluated aromatase activity. CYP19A1 knockdown notably decreased the ER activity (Fig. 3G). Besides, HPLC-MS was performed to measure the concentration of intracellular 17β-estradiol. As expected, the 17β-estradiol level was significantly increased after overexpressing CYP19A1 in PC3 cells (Fig. 3H). Furthermore, we found that androgen-independent PCa cell lines (PC3, LNCaP abl) showed significantly higher level of intracellular 17β-estradiol and ER activity compare with androgen-dependent PCa cell lines (LNCaP, Fig. S3). In addition, in LNCaP and LNCaP abl cells, the intracellular 17β-estradiol level and ER activity were significantly higher in $CD44^+$ cells than in the $CD44^-$ cells (Fig. 3I and J).

3.4. Aromatase upregulates MMP12 expression through ERα and promotes androgen-independent prostate cancer cell line invasion

Metastasis is one of the main contributors to the death of CRPC patients [29]. GSEA of $CYP19A1^{High}$ and $CYP19A1^{Low}$ prostate adenocarcinoma samples from the TCGA dataset revealed that signatures representative of epithelial-mesenchymal transition was enriched in the $CYP19A1^{High}$ expression phenotype (Fig. 4A). To characterize the differential gene expression profile of $CYP19A1^{High}$ and $CYP19A1^{Low}$ samples, heatmaps and hierarchical clustering were generated using Morpheus (Fig. S4). Some metastasis-related genes had significantly higher expression in $CYP19A1^{High}$ samples than in $CYP19A1^{Low}$ samples, and knocking down CYP19A1 in PC3 cells significantly decreased the expression of CD44 and Vimentin, as well as the epithelial-mesenchymal transition-related transcription factors Twist and Snail and invasion-related MMP enzymes (Fig. S5). Strikingly, we observed a dramatic decrease in the mRNA and protein expression of MMP12 following CYP19A1 reduction in LNCaP abl and PC3 cells (Fig. 4B), and overexpressing CYP19A1 significant increased the mRNA expression of MMP12 in LNCaP cells (Fig. S6).

We next detected a potential ERE binding site in the MMP12 promoter using a kit from Qiagen. A ChIP assay was performed to verify this prediction. Our finding indicates that exposure to estrogen stimulated MMP12 transcription by inducing ERα binding to the specific ERE site in the MMP12 promoter region (Fig. 4C). In addition, knocking down CYP19A1 and MMP12 or treatment with ER inhibitor, ICI182780,

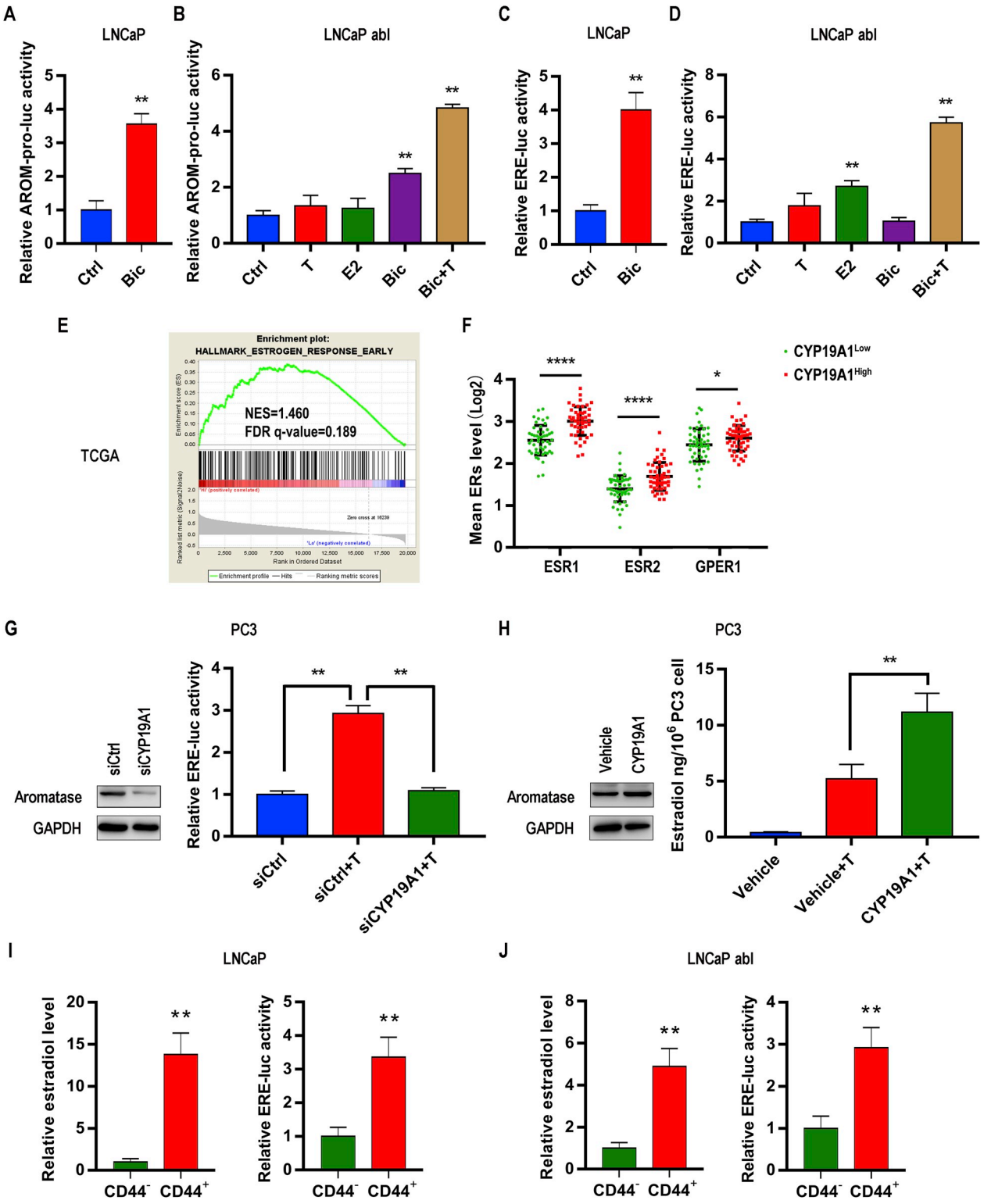

Fig. 3. Assessment of the estrogenic effects of bicalutamide treatment. (A–D) Relative aromatase promoter activity (AROM-pro-luc; A, B) and estrogen receptor (ER) transcriptional activity (ERE-luc; C, D) in LNCaP (*t*-test) and LNCaP abl (one-way ANOVA) cells after different treatment. (E) GSEA plot of the association between the early estrogen response gene set and *CYP19A1* in PRAD from TCGA. (F) Mean mRNA analysis of ERs for CYP19A1^{High} samples vs. CYP19A1^{Low} samples in PRAD from TCGA. (G) The protein levels of aromatase in PC3 cells transfected with siCtrl and siCYP19A1 are shown in the left panel, and ER transcriptional activity in PC3 cells exposed to 10 nM testosterone (T), transfected with siCtrl or siCYP19A1 is shown in the right panel (*t*-test). (H) The protein levels of aromatase in PC3 cells transfected with vehicle and CYP19A1 plasmids are shown in the left panel, and the intracellular 17β-estradiol concentration in PC3 cells is shown in the right panel (*t*-test). (I–J) The concentration of intracellular 17β-estradiol and ER transcriptional activity in CD44$^+$ and CD44$^-$ subsets of LNCaP (I) and LNCaP abl (J) cells (*t*-test). All studies were repeated at least three times; the values are the means ± SE; $^*P < 0.05$, $^{**}P < 0.01$, $^{****}P < 0.0001$.

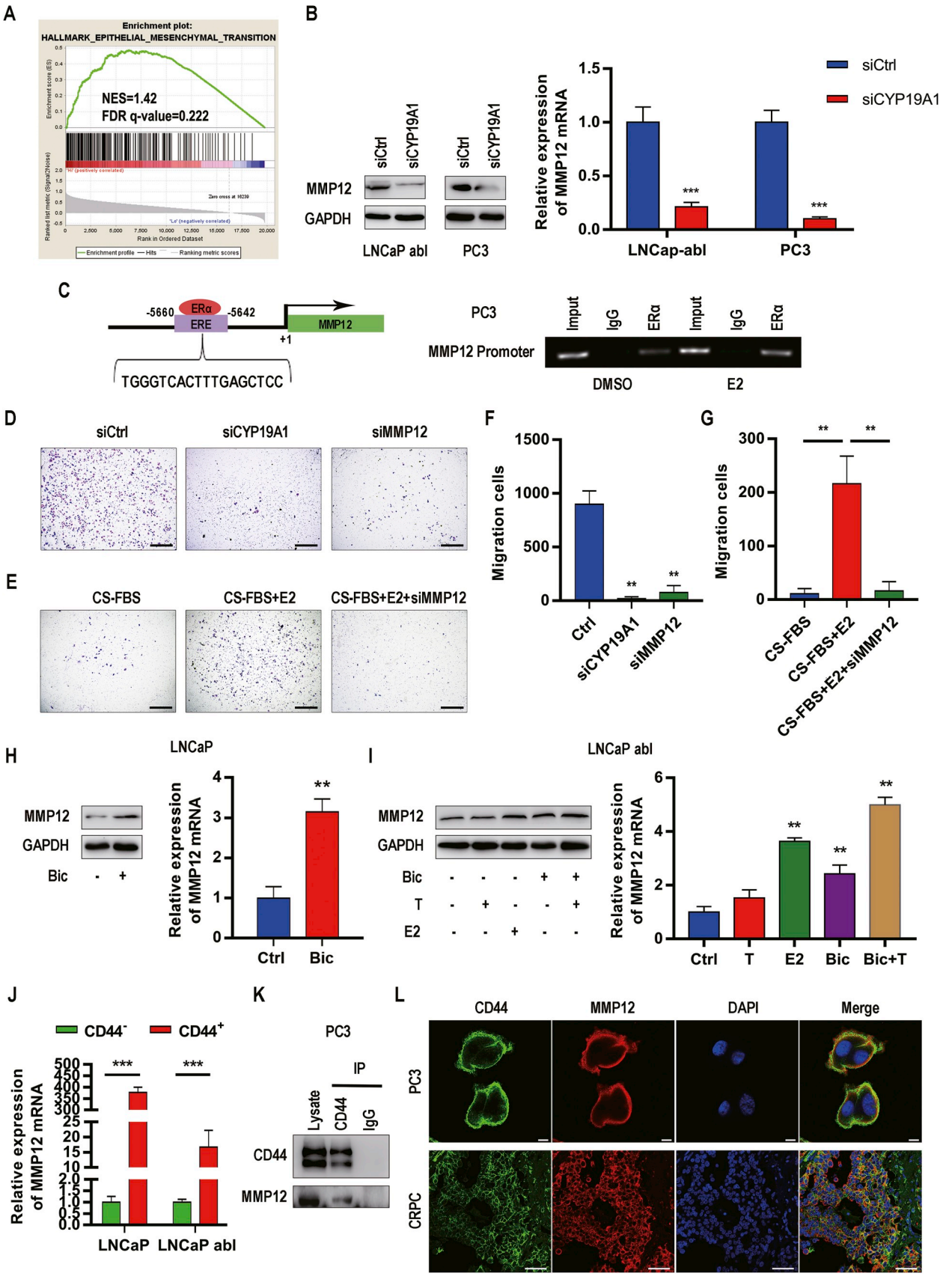

(caption on next page)

Fig. 4. Aromatase could promote PCa cell invasion *in vitro*. (A) GSEA plot of the association between the epithelial-mesenchymal transition gene set and *CYP19A1* in PRAD from TCGA. (B) MMP12 protein (left panel) and mRNA (right panel) levels in LNCaP abl and PC3 cells transfected with siCtrl and siCYP19A1. (C) ChIP assay showing that ERα binds directly to the ERE site of the MMP12 promoter region. (D and F) Invasion capability was assayed in PC3 cells transfected with siCYP19A1, siMMP12 and siCtrl (D), scale bar: 500 μm; F shows the quantitative results (one-way ANOVA). (E and G) Invasion capability was assayed in PC3 cells cultured in CS-FBS and exposed to 17β-estradiol after transfection with siMMP12 (E), scale bar: 500 μm. G shows the quantitative results (*t*-test). (H and I) MMP12 mRNA (left panel) and protein (right panel) levels in LNCaP (H, *t*-test) and LNCaP abl cells (I, one-way ANOVA) after treatment with bicalutamide. (J) *MMP12* mRNA expression in the $CD44^+$ vs. $CD44^-$ subsets of LNCaP and LNCaP abl cells by RT-PCR (*t*-test). (K) Co-IP assay showing that CD44 interacts with MMP12 in PC3 cells. (L) Representative immunofluorescence graphs of MMP12 and CD44 in PC3 cells (scale bar: 10 μm) and CRPC tissue (scale bar: 50 μm). All studies were repeated at least three times; the values are the means ± SE; $^*P < 0.05$, $^{**}P < 0.01$, $^{***}P < 0.001$; ChIP, chromatin immunoprecipitation; CS-FBS, charcoal-stripped foetal bovine serum; Co-IP, co-immunoprecipitation; IP, immunoprecipitation.

significantly decreased PC3 cell invasiveness (Fig. 4D and F and Figs. S7, S8, S9). When cultured in hormone-free conditions (CS-FBS), 17β-estradiol treatment enhanced the invasion of PC3 cells, but MMP12 knockdown dampened this effect (Fig. 4E and G).

Moreover, we observed mesenchymal-like morphological changes after treatment with bicalutamide in LNCaP and LNCaP abl cells (Fig. S10), and staining for E-cadherin, a calcium-dependent cell-cell adhesion protein, was also decreased (Fig. S11). Next, we examined the expression of MMP12 after bicalutamide treatment in LNCaP and LNCaP abl cells. The protein and mRNA levels of MMP12 were significantly increased after bicalutamide treatment (Fig. 4H and I).

As described earlier, aromatase is positively related to CD44 in PCa. Similarly, we found significantly higher *MMP12* expression in $CD44^+$ cells than in $CD44^-$ cells for both LNCaP and LNCaP abl cell lines (Fig. 4J) and androgen-independent PCa cells (LNCaP abl and PC3) showed significantly higher *MMP12* mRNA expression than was observed in androgen-dependent PCa cells (LNCaP, Fig. S12). It has been reported that MMPs (MMP9 and MT1-MMP) mediate cancer migration by interacting with CD44 [52,53]. To determine whether MMP12 could interact with CD44 in PCa cells, we performed Co-IP experiments. An anti-CD44 antibody specifically co-immunoprecipitated MMP12 in PC3 cells (Fig. 4K). This finding was confirmed by confocal microscopy, which showed that MMP12 and CD44 were co-localized on the cell membrane in PC3 cells (Fig. 4L). Moreover, we observed good colocalization of CD44 and MMP12 in CRPC tissue (Fig. 4L).

3.5. The aromatase inhibitor letrozole increased overall survival and inhibited tumour metastasis in castrated PC3 xenograft mice

In vitro studies suggested that aromatase promotes CRPC metastasis via MMP12. Furthermore, we established a castrated PC3-ZsGreen xenograft mouse model to determine whether aromatase influences tumour metastasis *in vivo* (Fig. 5A). Letrozole, an aromatase inhibitor, is widely used in cancers linked to estrogen, such as breast cancer [54]. In PC3 cells, we observed a dramatic time-dependent decrease in *MMP12* transcript levels following treatment with 50 nM letrozole (Fig. 5B). Here, testosterone (T), an aromatase substrate, 17β-estradiol (E2) and letrozole were used to evaluate the role of aromatase and estrogenic effects during the development of CRPC mouse xenografts. After 30 days of treatment, we observed a better overall survival and significantly higher body weight in the 2 groups treated with letrozole (LE and LE + T groups) than in the Ctrl group (Table 1 and Fig. 5C). However, mice in the T and E2 groups showed significant weight loss compared with mice in the Ctrl group (Fig. 5C). Then, full necropsies of the mice were performed at the time of sacrifice, and we detected a wide distribution of metastases, particularly in the lymph nodes and bone, in mice bearing PC3 tumours (Table 1 and Fig. 5D). The 2 groups treated with letrozole developed fewer metastases than the Ctrl group (Table 1). ZsGreen protein-expressing tumours were detected in both groups of mice using an imaging device after 30 days of treatment. The LE and LE + T groups showed significantly lower fluorescence intensity than the Ctrl group, while the fluorescence intensity in the T and E2 groups was significantly increased (Fig. 5E). Furthermore, primary tumours and metastases were stained with antibodies specific for aromatase, CD44 and MMP12. The groups of tumours treated with letrozole showed lower levels of aromatase CD44 and MMP12 than the other 3 groups of tumours (Fig. 5F). In addition, we observed strong staining for aromatase, CD44 and MMP12 in mouse metastases derived from PC3 cells (Fig. 5F and Fig. S13). Moreover, aromatase, CD44 and MMP12 showed good co-expression in PC3 tumours (Fig. S14).

4. Discussion

Aromatase has been demonstrated as a critical target in the management of women's cancers (breast, endometrium and ovarian) [55]. In benign prostate tissue, aromatase is expressed predominantly in the stroma; however, once it becomes malignant, aromatase expression has been detected in epithelial cells [56]. In this study, we found that the expression of aromatase is significantly increased in CRPC tissues and androgen-independent PCa cell lines. A subset of PCa patients with higher *CYP19A1* expression had a poorer overall survival after first hormone therapy than those with lower *CYP19A1* expression. Bicalutamide treatment increases aromatase expression and ER transcriptional activity in PCa cell lines. Additionally, *CYP19A1* expression was positively correlated with signatures representative of early estrogen response and epithelial-mesenchymal transition. In PC3 cells, CYP19A1 overexpression increased the concentration of endogenous estrogen, while CYP19A1 knockdown reduced the activity of ER, inhibited cell invasion and decreased the expression of some metastasis-related genes.

Previous studies suggest that PCSLCs are a critical contributor to CRPC [11]. In fact, $CD44^+$ stem-like cells are increased with PCa progression after ADT and might be initiators of EMT in a TRAMP mouse model [57]. Here, our data showed that aromatase is expressed predominantly in $CD44^+$ PCa cells which harboured more endogenous estrogen and stronger ER transcriptional activity compared with $CD44^+$ PCa cells, and co-expression of CD44 and aromatase was found in CRPC tissues and PCa cell lines. Moreover, the upregulation of aromatase expression after bicalutamide treatment is associated with the enrichment of the $CD44^+$ subset of cells, suggesting that the aberrant expression of aromatase in PCSLCs is involved in the development of CRPC.

To assess the feasibility of using aromatase as a therapeutic target for the treatment of CRPC, we established a castrated prostate cancer mouse model. Treatment with the aromatase inhibitor letrozole significantly increased overall survival and inhibited tumour metastasis in castrated PC3 xenograft mice. As early as the 1980s, a few small-scale clinical trials have attempted to employ aromatase inhibitors for the treatment of advanced PCa or CRPC. However, disparate results have been reported in these studies. The administration of aminoglutethimide appears to be a valuable second-line therapy for patients with androgen-independent and/or advanced PCa [58,59], but anastrozole and letrozole have not been shown to be active [60,61]. PCa clearly displays a remarkable degree of histologic and molecular heterogeneity. Zhao et al. segregated PCa into 3 subtypes: luminal A, luminal B and basal, which exhibit different clinical prognoses in response to ADT. Notably, patients with the basal subtype who had the highest ERα expression had poorer distant metastasis-free survival after ADT treatment than untreated patients [62]. In this study, we indicate that aromatase is co-expressed with CD44 in CRPC, suggesting that CRPC patients, who display basal or stem features, may benefit more from

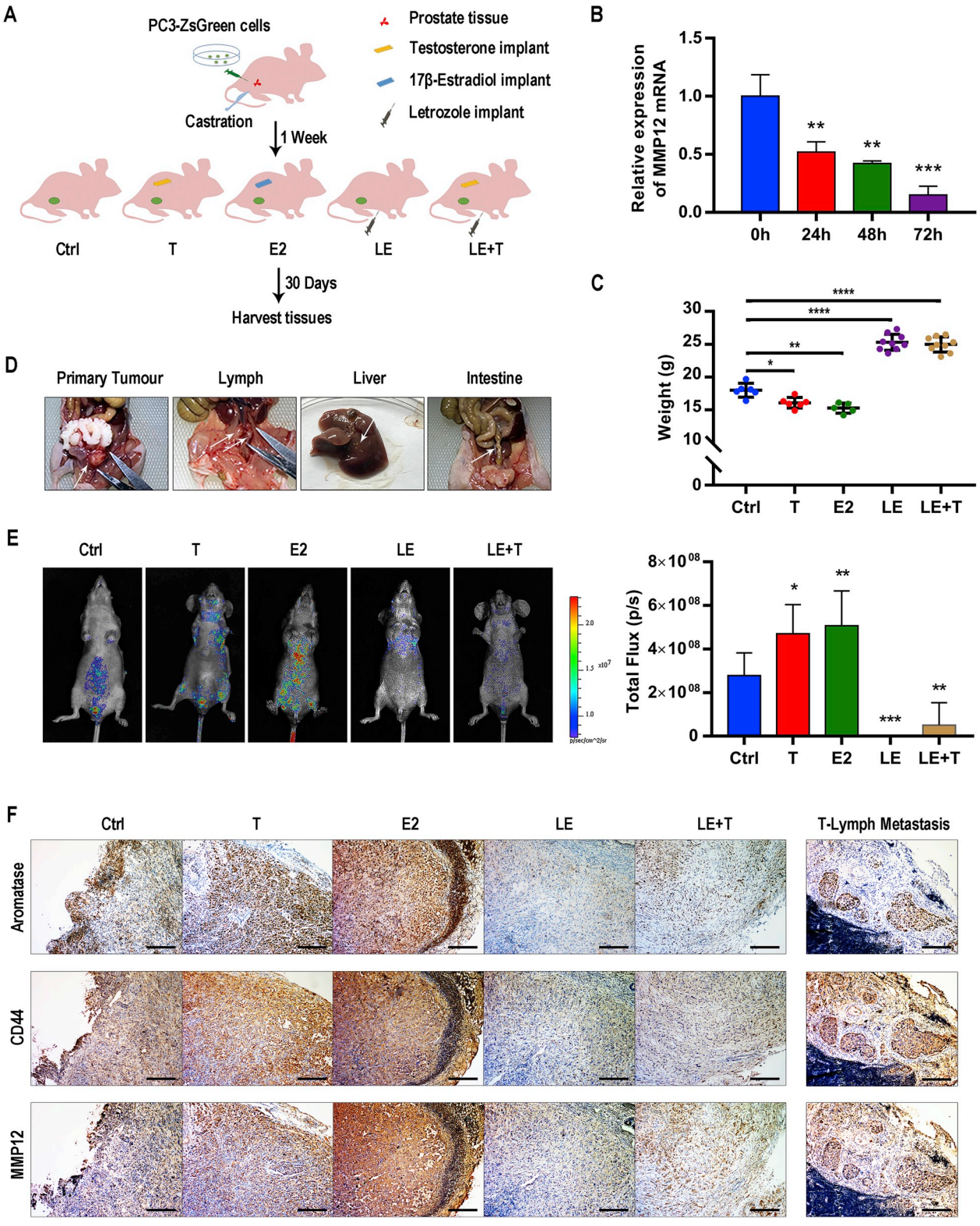

Fig. 5. Targeting aromatase inhibits tumour metastasis in CRPC mouse xenografts. (A) Schematic illustration of the experimental strategy. (B) PC3 cells were treated with 50 nM letrozole for 0 h, 24 h, 48 h and 72 h, and the mRNA expression level of *MMP12* was assayed by RT-PCR. (C) Body weights in mice with castration only (Ctrl, n = 6), castration plus testosterone (T, n = 6), castration plus estradiol (E2, n = 5), castration plus the aromatase inhibitor letrozole (LE, n = 9) and castration plus testosterone plus letrozole (LE + T, n = 9) before sacrifice. (D) Primary tumour and metastases in PC3 xenograft mice; the white arrows indicate PC3 tumours. (E) Representative images of *in vivo* bioluminescent imaging for mice in the 5 groups using the IVIS imaging system. The total fluorescence intensity (total flux) of the 5 groups is quantified on the right. (F) Representative images of the tumours immunostained with antibodies against aromatase, CD44 and MMP12, scale bar: 200 μm. The values are the means ± SE; $^{*}P < 0.05$ $^{**}P < 0.01$, $^{***}P < 0.001$, $^{****}P < 0.0001$.

Table 1
Mortality and metastasis rates in the PC3 xenograft mouse model.

Survival rate	Ctrl (n = 9)	T (n = 9)	E2 (n = 9)	LE (n = 9)	LE + T (n = 9)
	6 (66.7%)	6 (66.7%)	5 (55.6%)	9 (100.0%)	9 (100.0%)
Metastasis rate					
Lymph	6 (100.0%)	6 (100.0%)	5 (100.0%)	3 (33.3%)	2 (22.2%)
Bone	3 (50.0%)	5 (83.3%)	4 (80.0%)	2 (22.2%)	2 (22.2%)
Liver	2 (33.3%)	1 (16.7%)	1 (20.0%)	ND	ND
Intestine	3 (50.0%)	ND	3 (60.0%)	1 (11.1%)	2 (22.2%)
Spleen	1 (16.7%)	ND	3 (60.0%)	ND	ND
OMFR	1 (16.7%)	2 (33.3%)	3 (60.0%)	ND	ND

ND, not detected; OMFR, oral and maxillofacial region.

aromatase inhibitor treatment.

We further investigated the molecular mechanism by which aromatase promotes the metastasis of CRPC. Matrix metalloproteinases are the most prominent family of proteinases associated with tumourigenesis [30]. It has been reported that MMPs are upregulated in PCa tissues or blood from PCa patients [63]. Here, we detected that MMP12 expression is increased in CRPC patient tissues (Fig. S14), and MMP12 knockdown attenuates PC3 cell invasion. After bicalutamide treatment, MMP12 expression is significantly increased and is associated with higher aromatase expression in PCa cells. Furthermore, we found that endogenous estrogen produced by aromatase upregulates MMP12 expression via ERα. These data suggest that upregulating MMP12 expression may be a crucial mechanism by which aromatase promotes CRPC metastasis.

In the present study, we also found that MMP12 is expressed predominantly in the $CD44^+$ subset of LNCaP and LNCaP abl cells. By Co-IP and confocal microscopy, we revealed the interaction of CD44 and MMP12 on PCa cell membranes as well as in CRPC tissue. As a cell surface integral membrane protein, CD44 is considered not only to be a stem-like cell surface marker but also to be involved in tumour metastasis by interacting with appropriate extracellular matrix ligands, including osteopontin, collagens, and matrix MMPs [64]. The interaction between CD44 and MMP9 promotes cell migration and invasion in glioblastoma and anaplastic large cell lymphomas [53,65]. These reports suggest that the interaction of CD44 and MMP12 may be an effective mechanism involved in tumour metastasis; however, the role of interaction between CD44 and MMP12 in CRPC remains to be further explored in future studies.

In recent years, cumulative research efforts have revealed the contribution of persistent AR signalling to CRPC development [8]. Targeting androgen and ARs provides important benefits for CRPC treatment [66]; however, resistance still occurs [7]. In our work (Fig. 6), we demonstrate that CRPC harbours a significantly higher level of aromatase than primary PCa, suggesting the role of estrogen catalysed by a high level of aromatase in CRPC progression. In fact, increased endogenous estrogen catalysed by a high level of aromatase promotes tumour metastasis which is one of the main contributors to CRPC patient death [29]. In addition, our findings indicate that aromatase was expressed predominantly in $CD44^+$ PCSLCs which are considered critical contributors to PCa metastasis [57]. Targeting aromatase may be a promising therapy to inhibit the metastasis of CRPC induced by PCSLCs. In summary, our findings suggest that high aromatase expression and the resulting enhanced estrogenic effects might be one of the mechanisms underlying CRPC development. Combinatorial targeting of estrogen signals, for example, with aromatase inhibitors, and androgen signals may represent a unique therapeutic regimen for a subset of patients with CRPC.

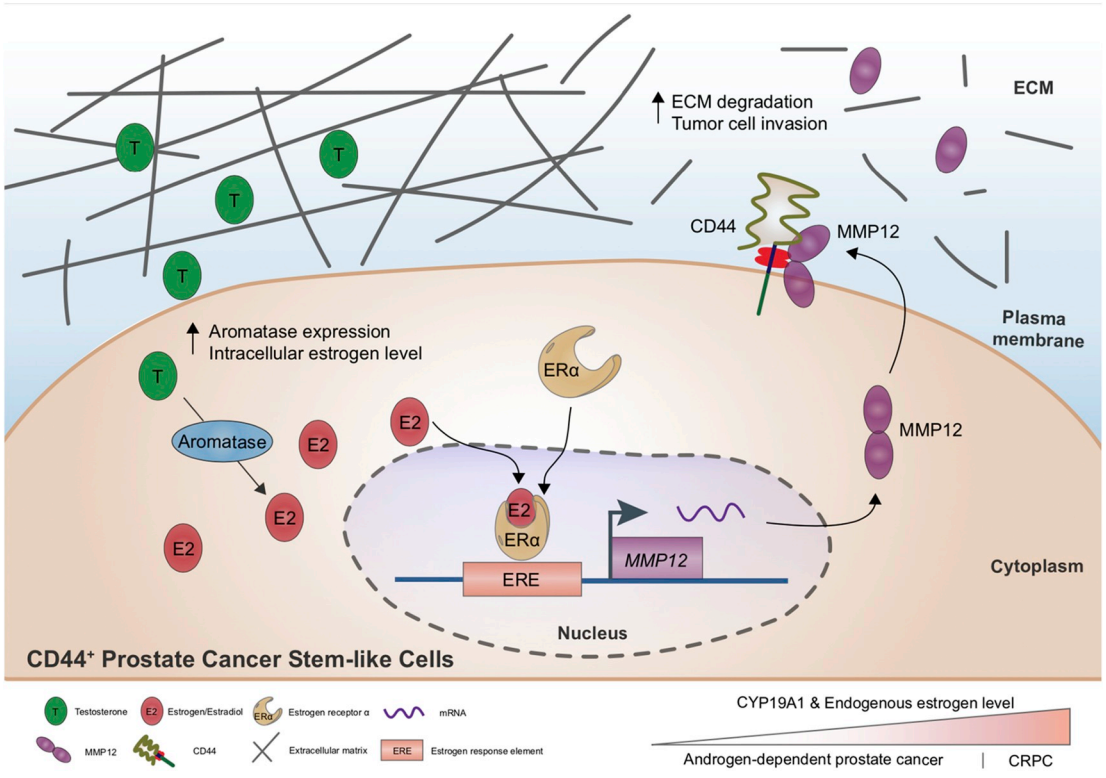

Fig. 6. Proposed mechanism of aromatase and intracellular estrogen role in $CD44^+$ prostate cancer stem-like cells and CRPC metastasis. In prostate cancer, CRPC harbour higher aromatase protein and intracellular estrogen levels compared with androgen-dependent prostate cancer. Aromatase is predominantly expressed in $CD44^+$ prostate cancer stem-like cells. The intracellular estrogen induced by aromatase promotes ERα binding to the ERE site of the MMP12 promoter region and enhances MMP12 expression. Secreted MMP12 co-localized with CD44 on the cell membrane and promotes tumour cell invasion.

Conflicts of interest

The authors declare that they have no competing interests.

Authors' contributions

ZX.L. designed and conducted the study, analysed the data and drafted the manuscript. JS.C. designed the study and completed bioinformatics analysis. L.T. completed the bioinformatics analysis. YM.S., X.Y., QM.L. and R.Z. conducted the study, HT.L. and XL.D. provided study materials, and J.Z. and JD.S. provided study materials and helped to draft the manuscript. All authors read and approved the final manuscript.

Acknowledgements and funding

This work was completely supported by grants from the National Natural Science Foundation of China (No. 81672527, No. 81872087, No. 81572784 and No. 81772687).

Appendix A. Supplementary data

Supplementary data to this article can be found online at https://doi.org/10.1016/j.canlet.2019.09.001.

References

[1] R.L. Siegel, K.D. Miller, A. Jemal, Cancer statistics, 2018, CA Cancer J. Clin. 68 (1) (2018) 7–30.
[2] C. Huggins, C.V. Hodges, Studies on prostatic cancer. I. The effect of castration, of estrogen and androgen injection on serum phosphatases in metastatic carcinoma of the prostate, CA Cancer J. Clin. 22 (4) (1972) 232–240.
[3] E.D. Crawford, P.F. Schellhammer, D.G. McLeod, J.W. Moul, C.S. Higano, N. Shore, et al., Androgen receptor targeted treatments of prostate cancer: 35 Years of progress with Antiandrogens, J. Urol. 200 (5) (2018) 956–966.
[4] A. Heidenreich, P.J. Bastian, J. Bellmunt, M. Bolla, S. Joniau, T. van der Kwast, et al., EAU guidelines on prostate cancer. Part II: treatment of advanced, relapsing, and castration-resistant prostate cancer, Eur. Urol. 65 (2) (2014) 467–479.
[5] T. Karantanos, P.G. Corn, T.C. Thompson, Prostate cancer progression after androgen deprivation therapy: mechanisms of castrate resistance and novel therapeutic approaches, Oncogene 32 (49) (2013) 5501–5511.
[6] J.S. de Bono, C.J. Logothetis, A. Molina, K. Fizazi, S. North, L. Chu, et al., Abiraterone and increased survival in metastatic prostate cancer, N. Engl. J. Med. 364 (21) (2011) 1995–2005.
[7] P.A. Watson, V.K. Arora, C.L. Sawyers, Emerging mechanisms of resistance to androgen receptor inhibitors in prostate cancer, Nat. Rev. Cancer 15 (12) (2015) 701–711.
[8] T. Karantanos, C.P. Evans, B. Tombal, T.C. Thompson, R. Montironi, W.B. Isaacs, Understanding the mechanisms of androgen deprivation resistance in prostate cancer at the molecular level, Eur. Urol. 67 (3) (2015) 470–479.
[9] M. Puhr, J. Hoefer, A. Eigentler, C. Ploner, F. Handle, G. Schaefer, et al., The glucocorticoid receptor is a key player for prostate cancer cell survival and a target for improved Antiandrogen therapy, Clin. Cancer Res. 24 (4) (2018) 927–938.
[10] F.R. Santer, H.H. Erb, R.V. McNeill, Therapy escape mechanisms in the malignant prostate, Semin. Cancer Biol. 35 (2015) 133–144.
[11] D. Ojo, X. Lin, N. Wong, Y. Gu, D. Tang, Prostate cancer stem-like cells contribute to the development of castration-resistant prostate cancer, Cancers (Basel) 7 (4) (2015) 2290–2308.
[12] Y. Yin, L. Xu, Y. Chang, T. Zeng, X. Chen, A. Wang, et al., N-Myc promotes therapeutic resistance development of neuroendocrine prostate cancer by differentially regulating miR-421/ATM pathway, Mol. Cancer 18 (1) (2019) 11.
[13] S.O. Lee, Z. Ma, C.R. Yeh, J. Luo, T.H. Lin, K.P. Lai, et al., New therapy targeting differential androgen receptor signaling in prostate cancer stem/progenitor vs. non-stem/progenitor cells, J. Mol. Cell Biol. 5 (1) (2013) 14–26.
[14] W.Y. Hu, G.B. Shi, H.M. Lam, D.P. Hu, S.M. Ho, I.C. Madueke, et al., Estrogen-initiated transformation of prostate epithelium derived from normal human prostate stem-progenitor cells, Endocrinology 152 (6) (2011) 2150–2163.
[15] S.J. Ellem, G.P. Risbridger, Treating prostate cancer: a rationale for targeting local oestrogens, Nat. Rev. Cancer 7 (8) (2007) 621–627.
[16] H. Bonkhoff, Estrogen receptor signaling in prostate cancer: implications for carcinogenesis and tumor progression, The Prostate 78 (1) (2018) 2–10.
[17] H.P. Rahman, J. Hofland, P.A. Foster, In touch with your feminine side: how oestrogen metabolism impacts prostate cancer, Endocr. Relat. Cancer 23 (6) (2016) R249–R266.
[18] D.P. Rose, K. Laakso, M. Sotarauta, E.L. Wynder, Hormone levels in prostatic fluid from healthy finns and prostate cancer patients, Eur. J. Cancer Clin. Oncol. 20 (10) (1984) 1317–1319.
[19] D. Chakravarty, A. Sboner, S.S. Nair, E. Giannopoulou, R.H. Li, S. Hennig, et al., The oestrogen receptor alpha-regulated lncRNA NEAT1 is a critical modulator of prostate cancer, Nat. Commun. 5 (2014) 16.
[20] S.R. Setlur, K.D. Mertz, Y. Hoshida, F. Demichelis, M. Lupien, S. Perner, et al., Estrogen-dependent signaling in a molecularly distinct subclass of aggressive prostate cancer, J. Natl. Cancer Inst. 100 (11) (2008) 815–825.
[21] M.M. Regan, P. Neven, A. Giobbie-Hurder, A. Goldhirsch, B. Ejlertsen, L. Mauriac, et al., Assessment of letrozole and tamoxifen alone and in sequence for postmenopausal women with steroid hormone receptor-positive breast cancer: the BIG 1-98 randomised clinical trial at 8.1 years median follow-up, Lancet Oncol. 12 (12) (2011) 1101–1108.
[22] D. Gianfrilli, S. Pierotti, R. Pofi, C. Leonardo, M. Ciccariello, F. Barbagallo, Sex steroid metabolism in benign and malignant intact prostate biopsies: individual profiling of prostate intracrinology, BioMed Res. Int. (2014) 464869 2014.
[23] F. Modugno, J.L. Weissfeld, D.L. Trump, J.M. Zmuda, P. Shea, J.A. Cauley, et al., Allelic variants of aromatase and the androgen and estrogen receptors: toward a multigenic model of prostate cancer risk, Clin. Cancer Res. 7 (10) (2001) 3092–3096.
[24] R. Miftakhova, A. Hedblom, J. Semenas, B. Robinson, A. Simoulis, J. Malm, et al., Cyclin A1 and P450 aromatase promote metastatic homing and growth of stem-like prostate cancer cells in the bone marrow, Cancer Res. 76 (8) (2016) 2453–2464.
[25] M. Zoller, CD44: can a cancer-initiating cell profit from an abundantly expressed molecule? Nat. Rev. Cancer 11 (4) (2011) 254–267.
[26] C. Liu, K. Kelnar, B.G. Liu, X. Chen, T. Calhoun-Davis, H.W. Li, et al., The microRNA miR-34a inhibits prostate cancer stem cells and metastasis by directly repressing CD44, Nat. Med. 17 (2) (2011) 211-U105.
[27] L. Patrawala, T. Calhoun, R. Schneider-Broussard, H. Li, B. Bhatia, S. Tang, et al., Highly purified CD44+ prostate cancer cells from xenograft human tumors are enriched in tumorigenic and metastatic progenitor cells, Oncogene 25 (12) (2006) 1696–1708.
[28] E.J. Yun, J. Zhou, C.J. Lin, E. Hernandez, L. Fazli, M. Gleave, et al., Targeting cancer stem cells in castration-resistant prostate cancer, Clin. Cancer Res. 22 (3) (2016) 670–679.
[29] D.M. Moreira, L.E. Howard, K.N. Sourbeer, H.S. Amarasekara, L.C. Chow, D.C. Cockrell, et al., Predictors of time to metastasis in castration-resistant prostate cancer, Urology 96 (2016) 171–176.
[30] K. Kessenbrock, V. Plaks, Z. Werb, Matrix metalloproteinases: regulators of the tumor microenvironment, Cell 141 (1) (2010) 52–67.
[31] S. Sarkar, R.K. Nuttall, S. Liu, D.R. Edwards, V.W. Yong, Tenascin-C stimulates glioma cell invasion through matrix metalloproteinase-12, Cancer Res. 66 (24) (2006) 11771–11780.
[32] I.C. Chung, L.C. Chen, A.K. Chung, M. Chao, H.Y. Huang, C. Hsueh, et al., Matrix metalloproteinase 12 is induced by heterogeneous nuclear ribonucleoprotein K and promotes migration and invasion in nasopharyngeal carcinoma, BMC Canc. 14 (2014).
[33] S.M. Nabha, E.B. dos Santos, H.A. Yamamoto, A. Belizi, Z. Dong, H. Meng, et al., Bone marrow stromal cells enhance prostate cancer cell invasion through type I collagen in an MMP-12 dependent manner, Int. J. Cancer 122 (11) (2008) 2482–2490.
[34] H. Ross-Adams, A.D. Lamb, M.J. Dunning, S. Halim, J. Lindberg, C.M. Massie, et al., Integration of copy number and transcriptomics provides risk stratification in prostate cancer: a discovery and validation cohort study, EBioMedicine 2 (9) (2015) 1133–1144.
[35] S.A. Tomlins, R. Mehra, D.R. Rhodes, X. Cao, L. Wang, S.M. Dhanasekaran, et al., Integrative molecular concept modeling of prostate cancer progression, Nat. Genet. 39 (1) (2007) 41–51.
[36] Y.P. Yu, D. Landsittel, L. Jing, J. Nelson, B. Ren, L. Liu, et al., Gene expression alterations in prostate cancer predicting tumor aggression and preceding development of malignancy, J. Clin. Oncol. 22 (14) (2004) 2790–2799.
[37] C.S. Grasso, Y.M. Wu, D.R. Robinson, X. Cao, S.M. Dhanasekaran, A.P. Khan, et al., The mutational landscape of lethal castration-resistant prostate cancer, Nature 487 (7406) (2012) 239–243.
[38] P. Ekambaram, J.L. Lee, N.E. Hubel, D. Hu, S. Yerneni, P.G. Campbell, et al., The CARMA3-Bcl10-MALT1 signalosome drives NFkappaB activation and promotes aggressiveness in Angiotensin II receptor-positive breast cancer, Cancer Res. 78 (5) (2018) 1225–1240.
[39] M.D. Robinson, D.J. McCarthy, G.K. Smyth, edgeR: a Bioconductor package for differential expression analysis of digital gene expression data, Bioinformatics 26 (1) (2010) 139–140.
[40] H.H. Chen, Y.C. Chiu, T. Zhang, S. Zhang, Y. Huang, Y. Chen, GSAE: an autoencoder with embedded gene-set nodes for genomics functional characterization, BMC Syst. Biol. 12 (Suppl 8) (2018) 142.
[41] B. Jia, Y. Gao, M. Li, J. Shi, Y. Peng, X. Du, et al., GPR30 promotes prostate stromal cell activation via suppression of ERalpha expression and its downstream signaling pathway, Endocrinology 157 (8) (2016) 3023–3035.
[42] Y.F. Peng, R. Zhang, L.F. Kong, Y.M. Shen, D. Xu, F. Zheng, et al., Ginsenoside Rg3 inhibits the senescence of prostate stromal cells through down-regulation of interleukin 8 expression, Oncotarget 8 (39) (2017) 64779–64792.
[43] C. Meng, Z. Lu, M. Fang, X. Zhou, K. Dai, S. Zhang, et al., Effect of celecoxib combined with chemotherapy drug on malignant biological behaviors of gastric cancer, Int. J. Clin. Exp. Pathol. 7 (11) (2014) 7622–7632.
[44] Z.S. Zhang, L. Duan, X.L. Du, H.S. Ma, I. Park, C. Lee, et al., The proliferative effect of estradiol on human prostate stromal cells is mediated through activation of ERK, The Prostate 68 (5) (2008) 508–516.
[45] Q. Wu, J.D. Shi, L.F. Chen, C.Y. Wang, I. Park, C. Lee, et al., Regulation of proliferation and differentiation of prostatic stromal cells by oestradiol through

prostatic epithelial cells in a paracrine manner, BJU Int. 101 (4) (2008) 497–502.
[46] C.Y. Wang, J.D. Shi, C.H. Yan, Q. Wu, H. Klocker, I. Park, et al., Development of a cell-isolation method for human prostatic smooth muscle cells based on cell type-specific activation of the SM22 gene promoter, BJU Int. 99 (1) (2007) 183–188.
[47] H.J. Huang, P.H. Chiang, S.H. Chen, Quantitative analysis of estrogens and estrogen metabolites in endogenous MCF-7 breast cancer cells by liquid chromatography-tandem mass spectrometry, J. Chromatogr. B Analyt. Technol. Biomed. Life Sci. 879 (20) (2011) 1748–1756.
[48] Y. Peng, J. Shi, X. Du, L. Wang, H. Klocker, L. Mo, et al., Prostaglandin E2 induces stromal cell-derived factor-1 expression in prostate stromal cells by activating protein kinase A and transcription factor Sp1, Int. J. Biochem. Cell Biol. 45 (3) (2013) 521–530.
[49] R. Yang, Y.X. Ma, L.F. Chen, Y. Zhou, Z.P. Yang, Y. Zhu, et al., Antagonism of estrogen-mediated cell proliferation by raloxifene in prevention of ageing-related prostatic hyperplasia, Asian J. Androl. 12 (5) (2010) 735–743.
[50] S. Gupta, Y. Wang, R. Ramos-Garcia, D. Shevrin, J.B. Nelson, Z. Wang, Inhibition of 5alpha-reductase enhances testosterone-induced expression of U19/Eaf2 tumor suppressor during the regrowth of LNCaP xenograft tumor in nude mice, The Prostate 70 (14) (2010) 1575–1585.
[51] Z. Culig, J. Hoffmann, M. Erdel, I.E. Eder, A. Hobisch, A. Hittmair, et al., Switch from antagonist to agonist of the androgen receptor blocker bicalutamide is associated with prostate tumour progression in a new model system, Br. J. Canc. 81 (2) (1999) 242–251.
[52] W. Jiang, Y. Zhang, K.T. Kane, M.A. Collins, D.M. Simeone, M.P. di Magliano, et al., CD44 regulates pancreatic cancer invasion through MT1-MMP, Mol. Cancer Res. 13 (1) (2015) 9–15.
[53] C. Chetty, S.K. Vanamala, C.S. Gondi, D.H. Dinh, M. Gujrati, J.S. Rao, MMP-9 induces CD44 cleavage and CD44 mediated cell migration in glioblastoma xenograft cells, Cell. Signal. 24 (2) (2012) 549–559.
[54] M. Colleoni, W. Luo, P. Karlsson, J. Chirgwin, S. Aebi, G. Jerusalem, et al., Extended adjuvant intermittent letrozole versus continuous letrozole in postmenopausal women with breast cancer (SOLE): a multicentre, open-label, randomised, phase 3 trial, Lancet Oncol. 19 (1) (2018) 127–138.
[55] S.E. Bulun, D. Chen, M. Lu, H. Zhao, Y. Cheng, M. Demura, et al., Aromatase excess in cancers of breast, endometrium and ovary, J. Steroid Biochem. Mol. Biol. 106 (1–5) (2007) 81–96.
[56] S.J. Ellem, J.F. Schmitt, J.S. Pedersen, M. Frydenberg, G.P. Risbridger, Local aromatase expression in human prostate is altered in malignancy, J. Clin. Endocrinol. Metab. 89 (5) (2004) 2434–2441.
[57] Z. Shang, Q. Cai, M. Zhang, S. Zhu, Y. Ma, L. Sun, et al., A switch from CD44(+) cell to EMT cell drives the metastasis of prostate cancer, Oncotarget 6 (2) (2015) 1202–1216.
[58] W.H. Kruit, G. Stoter, J.G. Klijn, Effect of combination therapy with aminoglutethimide and hydrocortisone on prostate-specific antigen response in metastatic prostate cancer refractory to standard endocrine therapy, Anti Canccer Drugs 15 (9) (2004) 843–847.
[59] B.A. Ponder, R.J. Shearer, R.D. Pocock, J. Miller, D. Easton, C.E. Chilvers, et al., Response to aminoglutethimide and cortisone acetate in advanced prostatic cancer, Br. J. Canc. 50 (6) (1984) 757–763.
[60] M.R. Smith, D. Kaufman, D. George, W.K. Oh, M. Kazanis, J. Manola, et al., Selective aromatase inhibition for patients with androgen-independent prostate carcinoma, Cancer 95 (9) (2002) 1864–1868.
[61] R.J. Santen, G.R. Petroni, M.J. Fisch, C.E. Myers, D. Theodorescu, R.B. Cohen, Use of the aromatase inhibitor anastrozole in the treatment of patients with advanced prostate carcinoma, Cancer 92 (8) (2001) 2095–2101.
[62] S.G. Zhao, S.L. Chang, N. Erho, M. Yu, J. Lehrer, M. Alshalalfa, et al., Associations of luminal and basal subtyping of prostate cancer with prognosis and response to androgen deprivation therapy, JAMA Oncol 3 (12) (2017) 1663–1672.
[63] E. Hadler-Olsen, J.O. Winberg, L. Uhlin-Hansen, Matrix metalloproteinases in cancer: their value as diagnostic and prognostic markers and therapeutic targets, Tumour. Biol. 34 (4) (2013) 2041–2051.
[64] L.T. Senbanjo, M.A. Chellaiah, CD44: a multifunctional cell surface adhesion receptor is a regulator of progression and metastasis of cancer cells, Front. Cell. Dev. Biol. 5 (2017) 18.
[65] F. Lagarrigue, S. Dupuis-Coronas, D. Ramel, G. Delsol, H. Tronchere, B. Payrastre, et al., Matrix metalloproteinase-9 is upregulated in nucleophosmin-anaplastic lymphoma kinase-positive anaplastic lymphomas and activated at the cell surface by the chaperone heat shock protein 90 to promote cell invasion, Cancer Res. 70 (17) (2010) 6978–6987.
[66] W.U. Shipley, W. Seiferheld, H.R. Lukka, P.P. Major, N.M. Heney, D.J. Grignon, et al., Radiation with or without Antiandrogen therapy in recurrent prostate cancer, N. Engl. J. Med. 376 (5) (2017) 417–428.